

# Measurement of the $^{235}\text{U}(n,f)$ cross section relative to the $^{10}\text{B}(n,\alpha)$ reaction with Micromegas detectors at the CERN n\_TOF facility: first results

*Veatriki Michalopoulou*<sup>1,2,\*</sup>, *Maria Diakaki*<sup>1</sup>, *Rosa Vlastou*<sup>1</sup>, *Michael Kokkoris*<sup>1</sup>, *Athanasios Stamatopoulos*<sup>1</sup>, *Andrea Tsinganis*<sup>2</sup>, *Zinovia Eleme*<sup>3</sup>, *Nikolas Patronis*<sup>3</sup>, *Jan Heyse*<sup>4</sup>, *Peter Schillebeeckx*<sup>4</sup>, *Laurent Tassan-Got*<sup>2,1,5</sup>, *Massimo Barbagallo*<sup>2,6</sup>, *Nicola Colonna*<sup>6</sup>, *Sebastian Urlass*<sup>7,2</sup>, *Daniela Macina*<sup>2</sup>, *Enrico Chiaveri*<sup>2,8</sup>, *Oliver Aberle*<sup>2</sup>, *Victor Alcayne*<sup>9</sup>, *Simone Amaducci*<sup>10,11</sup>, *Józef Andrzejewski*<sup>12</sup>, *Laurent Audouin*<sup>5</sup>, *Victor Babiano-Suarez*<sup>13</sup>, *Michael Bacak*<sup>2,14,15</sup>, *Samuel Bennett*<sup>8</sup>, *Eric Berthoumieux*<sup>15</sup>, *Jon Billowes*<sup>8</sup>, *Damir Bosnar*<sup>16</sup>, *Adam Brown*<sup>17</sup>, *Maurizio Busso*<sup>18,19</sup>, *Manuel Caamaño*<sup>20</sup>, *Luis Caballero-Ontanaya*<sup>13</sup>, *Francisco Calviño*<sup>21</sup>, *Marco Calviani*<sup>2</sup>, *Daniel Cano-Ott*<sup>9</sup>, *Adria Casanovas*<sup>21</sup>, *Francesco Cerutti*<sup>2</sup>, *Guillem Cortés*<sup>21</sup>, *Miguel Cortés-Giraldo*<sup>22</sup>, *Luigi Cosentino*<sup>10</sup>, *Sergio Cristallo*<sup>18,23</sup>, *Lucia-Anna Damone*<sup>6,24</sup>, *Paul-John Davies*<sup>8</sup>, *Mirco Dietz*<sup>25</sup>, *César Domingo-Pardo*<sup>13</sup>, *Rugard Dressler*<sup>26</sup>, *Quentin Ducasse*<sup>27</sup>, *Emmeric Dupont*<sup>15</sup>, *Ignacio Durán*<sup>20</sup>, *Beatriz Fernández-Domínguez*<sup>20</sup>, *Alfredo Ferrari*<sup>2</sup>, *Paolo Finocchiaro*<sup>10</sup>, *Kathrin Göbel*<sup>28</sup>, *Ruchi Garg*<sup>25</sup>, *Aleksandra Gawlik-Ramięga*<sup>12</sup>, *Simone Gilardoni*<sup>2</sup>, *Isabel Gonçalves*<sup>29</sup>, *Enrique González-Romero*<sup>9</sup>, *Carlos Guerrero*<sup>22</sup>, *Frank Gunsing*<sup>15</sup>, *Hideo Harada*<sup>30</sup>, *Stephan Heinitz*<sup>26</sup>, *David Jenkins*<sup>17</sup>, *Arnd Junghans*<sup>7</sup>, *Franz Käppeler*<sup>31</sup>, *Yacine Kadi*<sup>2</sup>, *Atsushi Kimura*<sup>30</sup>, *Ingrid Knapová*<sup>32</sup>, *Milan Krčička*<sup>32</sup>, *Deniz Kurtulgil*<sup>28</sup>, *Ion Ladarescu*<sup>13</sup>, *Claudia Lederer-Woods*<sup>25</sup>, *Helmut Leeb*<sup>14</sup>, *Jorge Lerendegui-Marco*<sup>22</sup>, *Sarah-Jane Lonsdale*<sup>25</sup>, *Alice Manna*<sup>33,34</sup>, *Trinitario Martínez*<sup>9</sup>, *Alessandro Masi*<sup>2</sup>, *Cristian Massimi*<sup>33,34</sup>, *Pierfrancesco Mastinu*<sup>35</sup>, *Mario Mastromarco*<sup>2,6</sup>, *Emilio-Andrea Maugeri*<sup>26</sup>, *Annamaria Mazzone*<sup>6,36</sup>, *Emilio Mendoza*<sup>9</sup>, *Alberto Mengoni*<sup>37,33</sup>, *Paolo Milazzo*<sup>38</sup>, *Federica Mingrone*<sup>2</sup>, *Javier Moreno-Soto*<sup>15</sup>, *Agatino Musumarra*<sup>10,39</sup>, *Alexandru Negret*<sup>40</sup>, *Ralf Nolte*<sup>27</sup>, *Francisco Ogállar*<sup>41</sup>, *Andreea Oprea*<sup>40</sup>, *Andreas Pavlik*<sup>42</sup>, *Jaroslav Perkowski*<sup>12</sup>, *Luciano Piersanti*<sup>18,23</sup>, *Cristina Petrone*<sup>40</sup>, *Elisa Pirovano*<sup>27</sup>, *Ignacio Porras*<sup>41</sup>, *Javier Praena*<sup>41</sup>, *José-Manuel Quesada*<sup>22</sup>, *Diego Ramos-Doval*<sup>5</sup>, *Thomas Rauscher*<sup>43,44</sup>, *René Reifarth*<sup>28</sup>, *Dimitri Rochman*<sup>26</sup>, *Carlo Rubbia*<sup>2</sup>, *Marta Sabaté-Gilarte*<sup>22,2</sup>, *Alok Saxena*<sup>45</sup>, *Dorothea Schumann*<sup>26</sup>, *Adhitya Sekhar*<sup>8</sup>, *Gavin Smith*<sup>8</sup>, *Nikolay Sosnin*<sup>8</sup>, *Peter Sprung*<sup>26</sup>, *Giuseppe Tagliente*<sup>6</sup>, *José Tain*<sup>13</sup>, *Ariel Tarifeño-Saldivia*<sup>21</sup>, *Benedikt Thomas*<sup>28</sup>, *Pablo Torres-Sánchez*<sup>41</sup>, *Jiri Ulrich*<sup>26</sup>, *Stanislav Valenta*<sup>32</sup>, *Gianni Vannini*<sup>33,34</sup>, *Vincenzo Variale*<sup>6</sup>, *Pedro Vaz*<sup>29</sup>, *Alberto Ventura*<sup>33</sup>, *Diego Vescovi*<sup>18</sup>, *Vasilis Vlachoudis*<sup>2</sup>, *Anton Wallner*<sup>46</sup>, *Philip-John Woods*<sup>25</sup>, *Tobias Wright*<sup>8</sup>, *Petar Žugec*<sup>16</sup>

The n\_TOF Collaboration ([www.cern.ch/ntof](http://www.cern.ch/ntof))

<sup>1</sup>National Technical University of Athens, Greece

<sup>2</sup>European Organization for Nuclear Research (CERN), Switzerland

<sup>3</sup>University of Ioannina, Greece

<sup>4</sup>European Commission, Joint Research Centre (JRC), Geel, Belgium

<sup>5</sup>Institut de Physique Nucléaire, CNRS-IN2P3, Univ. Paris-Sud, Université Paris-Saclay, F-91406 Orsay Cedex, France

<sup>6</sup>Istituto Nazionale di Fisica Nucleare, Sezione di Bari, Italy

<sup>7</sup>Helmholtz-Zentrum Dresden-Rossendorf, Germany

<sup>8</sup>University of Manchester, United Kingdom

<sup>9</sup>Centro de Investigaciones Energéticas Medioambientales y Tecnológicas (CIEMAT), Spain

<sup>10</sup>INFN Laboratori Nazionali del Sud, Catania, Italy

<sup>11</sup>Dipartimento di Fisica e Astronomia, Università di Catania, Italy

<sup>12</sup>University of Lodz, Poland

<sup>13</sup>Instituto de Física Corpuscular, CSIC - Universidad de Valencia, Spain

<sup>14</sup>TU Wien, Atominstitut, Stadionallee 2, 1020 Wien, Austria

<sup>15</sup>CEA Irfu, Université Paris-Saclay, F-91191 Gif-sur-Yvette, France

<sup>16</sup>Department of Physics, Faculty of Science, University of Zagreb, Zagreb, Croatia

<sup>17</sup>University of York, United Kingdom

<sup>18</sup>Istituto Nazionale di Fisica Nucleare, Sezione di Perugia, Italy

<sup>19</sup>Dipartimento di Fisica e Geologia, Università di Perugia, Italy

<sup>20</sup>University of Santiago de Compostela, Spain

<sup>21</sup>Universitat Politècnica de Catalunya, Spain

<sup>22</sup>Universidad de Sevilla, Spain

<sup>23</sup>Istituto Nazionale di Astrofisica - Osservatorio Astronomico di Teramo, Italy

<sup>24</sup>Dipartimento Interateneo di Fisica, Università degli Studi di Bari, Italy

<sup>25</sup>School of Physics and Astronomy, University of Edinburgh, United Kingdom

<sup>26</sup>Paul Scherrer Institut (PSI), Villigen, Switzerland

<sup>27</sup>Physikalisch-Technische Bundesanstalt (PTB), Bundesallee 100, 38116 Braunschweig, Germany

<sup>28</sup>Goethe University Frankfurt, Germany

<sup>29</sup>Instituto Superior Técnico, Lisbon, Portugal

<sup>30</sup>Japan Atomic Energy Agency (JAEA), Tokai-Mura, Japan

<sup>31</sup>Karlsruhe Institute of Technology, Campus North, IKP, 76021 Karlsruhe, Germany

<sup>32</sup>Charles University, Prague, Czech Republic

<sup>33</sup>Istituto Nazionale di Fisica Nucleare, Sezione di Bologna, Italy

<sup>34</sup>Dipartimento di Fisica e Astronomia, Università di Bologna, Italy

<sup>35</sup>Istituto Nazionale di Fisica Nucleare, Sezione di Legnaro, Italy

<sup>36</sup>Consiglio Nazionale delle Ricerche, Bari, Italy

<sup>37</sup>Agenzia nazionale per le nuove tecnologie (ENEA), Bologna, Italy

<sup>38</sup>Istituto Nazionale di Fisica Nucleare, Sezione di Trieste, Italy

<sup>39</sup>Dipartimento di Fisica e Astronomia, Università di Catania, Italy

<sup>40</sup>Horia Hulubei National Institute of Physics and Nuclear Engineering, Romania

<sup>41</sup>University of Granada, Spain

<sup>42</sup>University of Vienna, Faculty of Physics, Vienna, Austria

<sup>43</sup>Department of Physics, University of Basel, Switzerland

<sup>44</sup>Centre for Astrophysics Research, University of Hertfordshire, United Kingdom

<sup>45</sup>Bhabha Atomic Research Centre (BARC), India

<sup>46</sup>Australian National University, Canberra, Australia

**Abstract.** Neutron cross section measurements are often made relative to a neutron cross section standard. Thus, the accuracy of the neutron standards determines the best possible accuracy of the neutron measurements. The  $^{235}\text{U}(n,f)$  cross section is widely used as reference, while it is considered a standard at thermal point and between 0.15 to 200 MeV. For this reason, additional cross section data for the  $^{235}\text{U}(n,f)$  reaction are useful in order to improve the accuracy and to extend the energy range of the standard. In this work, preliminary results of the measurement of the  $^{235}\text{U}(n,f)$  cross-section relative to the standard  $^{10}\text{B}(n,\alpha)$  reaction are presented. The high accuracy measurement was performed at the experimental area EAR-1 of the n\_TOF facility at CERN, aiming at covering the energy range from the thermal region up to approximately 100 keV. The samples were produced at JRC-Geel in Belgium, while the experimental setup was based on Micromegas detectors.

## 1 Introduction

The  $^{235}\text{U}(n,f)$  reaction cross-section is a very important quantity for neutronic calculations of nuclear reactors and has been the subject of many experimental and theoretical works. Nevertheless, certain issues concerning this cross section have been pointed out, especially in the energy region below 100 keV [1-3]. In addition, it is widely used as reference in neutron-induced cross-section measurements, while it is considered a standard at the thermal point and in the energy range from 150 keV to 200 MeV [1]. However, in common practice, it is used as a reference reaction at a wide energy region, from thermal up to approximately 1 GeV [2, 4]. In order to improve the accuracy of the standard, as well as to extend the energy region where it is considered as such, additional measurements are required. In this framework a dedicated measurement has already been performed at the n\_TOF facility by Amaducci *et al.* [4, 5], implementing silicon detectors for the measurement.

In this work, the first results of a measurement performed with the gas detectors Micromegas relative to the standard  $^{10}\text{B}(n,\alpha)$  reaction, conducted at the neutron time-of-flight facility n\_TOF, located at CERN will be presented. This measurement aims at providing

additional high accuracy data using a different experimental setup in the same neutron facility.

## 2 Experimental setup

The measurement was performed at experimental area EAR-1 of the n\_TOF facility located at CERN. The neutrons are produced via the spallation of 20 GeV/c protons impinging on a Pb target, which leads to the creation of neutrons with energies ranging from thermal up to the GeV region. The distinction between the neutron energies is achieved with the time-of-flight technique, namely estimating the neutron energy by the time needed to reach the experimental area, considering the distance between the spallation target and the experimental area, which in the case of EAR-1 is 185 m.

For the detection of the fission fragments from the  $^{235}\text{U}(n,f)$  reaction and the alpha and  $^7\text{Li}$  nuclei from the  $^{10}\text{B}(n,\alpha)$  reaction, a setup based on Micromegas detectors [6-9] was used. The Micromegas detector is a gas detector divided into two parts: the drift region defined by the drift electrode, which is the sample itself ( $^{235}\text{U}$  or  $^{10}\text{B}$ ) and the mesh electrode, which is a thin Cu foil with 50  $\mu\text{m}$  holes and the amplification region defined between the mesh electrode and the anode electrode, a thin grounded Cu foil. A charged particle,

originating from the sample, enters the drift region and creates secondary electrons which drift towards the mesh, guided by the electric field. The electrons enter the amplification region where they encounter a higher electric field, leading to their amplification through avalanches. The signal is collected from the mesh electrode, using preamplifier modules constructed at INFN-Bari.

The samples were produced at JRC-Geel, and were deposited on thin foils with an areal density of  $8 \mu\text{g}/\text{cm}^2$  and  $72 \mu\text{g}/\text{cm}^2$  for the  $^{10}\text{B}$  and  $^{235}\text{U}$  sample respectively. The diameter of the samples was 8 cm, matching the diameter of the collimation system used in the experiments. The fission chamber, containing the Micromegas detectors and the actinide samples, which was placed at experimental EAR-1 is shown in Figure 1, while the preamplifier modules are placed on top of the chamber.

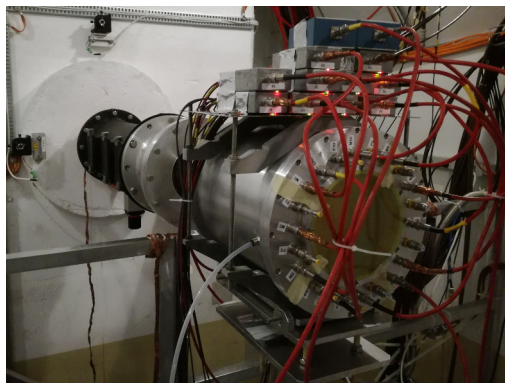


**Fig. 1.** The fission chamber containing the samples and the Micromegas detectors placed at experimental EAR-1 of the n\_TOF facility.

### 3 Data analysis

The detector waveforms were digitized and stored in order to be analysed by a pulse shape analysis routine [9]. The amplitude of each pulse is extracted from the analysis, as well as the time-of-flight, which is estimated relative to the “ $\gamma$ -flash” peak. The “ $\gamma$ -flash” is the first peak in the time-of-flight spectrum and contains signals from events of the spallation process, such as  $\gamma$ -rays, high-energy relativistic particles, as well as fission signals from high-energy neutrons. The timing of each pulse is estimated relative to the  $\gamma$ -flash peak.

An amplitude cut is introduced in the analysis in order to reject alpha particles from the natural radioactivity in the case of the  $^{235}\text{U}$  and noise for both samples. The clean amplitude spectrum for the  $^{235}\text{U}$  sample and for the  $^{10}\text{B}$  samples are presented in Figure 2 and Figure 3, respectively. The signals which are lost below the amplitude cut introduced in the analysis are estimated via FLUKA simulations [10], using the GEF code [11] as fission event generator in the case of the  $^{235}\text{U}$  sample and accounted for via the simulations. The simulated spectrum is then calibrated and convoluted with a skewed gaussian function in order to reproduce the experimental one. The experimental spectrum corresponding to neutron energies from 0.06 to 0.08 eV compared to the simulated one is presented in Figure 4

for the  $^{235}\text{U}$  sample, while the simulations are still ongoing for the  $^{10}\text{B}$  sample.

Additional corrections are required in order to extract the final results, which are in progress and include the correction for the counting losses, the correction for the contaminants present in the samples, the accurate determination of the flight path length taking into account the distance and time the neutrons spent inside the spallation target and the correction for the attenuation of the neutron beam.

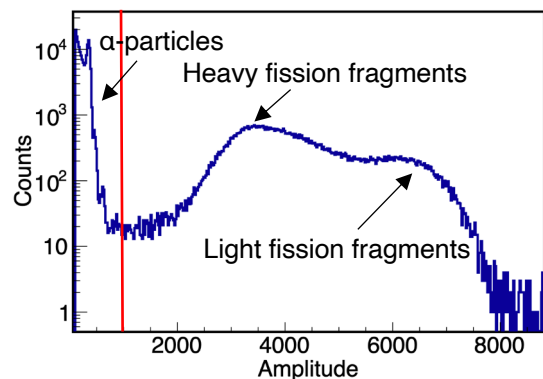


**Fig. 2.** Amplitude spectrum (in log scale) for the  $^{235}\text{U}$  sample corresponding to the energy range 0.025 to 0.03 eV. In this energy range the two peaks of the alpha particles from the alpha radioactivity of the sample are clearly formed, as well as the peaks from the heavy and light fission fragments. The red line represents the amplitude cut introduced in the analysis.

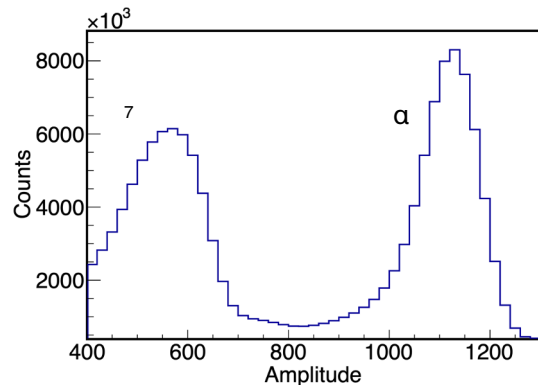


**Fig. 3.** Amplitude spectrum for the  $^{10}\text{B}$  sample, where the  $^7\text{Li}$  and alpha particle peaks are distinguished in the spectrum.

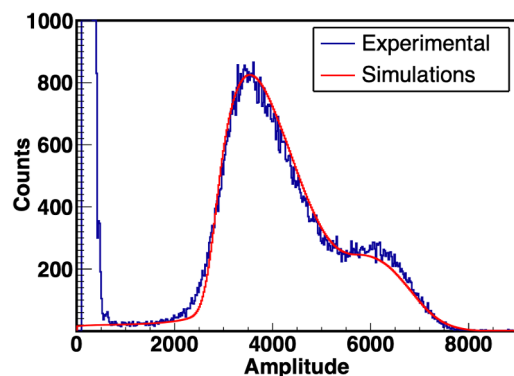


**Fig. 4.** Comparison of the experimental amplitude spectrum for neutron energies 0.06 to 0.08 eV (blue line) and simulated spectrum (red line) for the  $^{235}\text{U}$  sample.

## 4 Results

The preliminary cross-section values for the  $^{235}\text{U}(n,f)$  reaction estimated using the  $^{10}\text{B}(n,\alpha)$  reaction as reference and normalized to the ENDF/B-VIII.0 library [12] are presented in Figure 5. Only the statistical errors are shown in the figure, which are less than 5% for all neutron energies, with an isoenergic energy binning of 100 bins per decade.

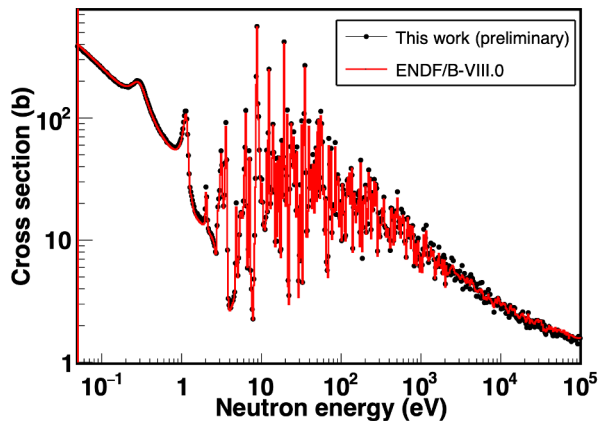


**Fig. 5.** Preliminary cross-section results for the  $^{235}\text{U}(n,f)$  reaction (black points) (with 100 bins per decade) in comparison with the evaluation of ENDF/B-VIII.0 [12]. The results are normalized to the evaluation.

As seen in the figure, the data from this work are in overall excellent agreement with the evaluation of ENDF/B-VIII.0. It is interesting to note here that structures are observed for energies higher than 2.25 keV, as also seen in the latest data of Amaducci et al. [4]. The data can assist in extending the Resolved Resonance Region beyond 2.25 keV.

## 5 Conclusions

A high resolution measurement of the  $^{235}\text{U}(n,f)$  cross-section with respect to the  $^{10}\text{B}(n,\alpha)$  reaction was performed at the experimental area EAR-1 of the n\_TOF facility at CERN. The analysis of the data is still ongoing, but the final results aim to assist in the improvement of the evaluations especially above 2.25 keV, where structures are observed in the experimental data, that are currently not taken into account as resonances in the existing evaluations. In addition, a theoretical investigation of the resonance parameters is foreseen to be performed in the framework of the R-matrix theory.

Funding from the European Union's Horizon 2020 research and innovation programme SANDA (Supplying Accurate Nuclear Data for energy and non-energy Applications) under grant agreement no 847552, is gratefully acknowledged.

In line with the principles that apply to scientific publishing and the CERN policy in matters of scientific publications, the n\_TOF Collaboration recognises the work of V. Furman and Y. Kopatch (JINR, Russia), who have contributed to the experiment used to obtain the results described in this paper.

## References

1. A. D. Carlson et al., Nucl. Data Sheets **148** (2018) 143
2. M. Barbagallo et al., Eur. Phys. J. A **49** (2013) 156
3. M. Jandel et al., Phys. Rev. Lett. **109** (2012) 202506
4. S. Amaducci et al., Eur. Phys. J. A **55**, **120** (2019)
5. M. Mastromarco et al., Eur. Phys. J. A **58**, 147 (2022)
6. L. Shekhtman, Nucl. Instrum. Meth. A **494**, 128 (2002)
7. Y. Giomataris, Nucl. Instrum. Meth. A **419**, 239 (1998)
8. S. Andriamonje et al., J. Instrum. **5**, P02001 (2010).
9. P. Žugec et al., Nucl. Instrum. Meth. A, **812**, 134 (2016)
10. T.T. Böhlen et al., Nucl. Data Sheets **120**, 211 (2014)
11. K.-H. Schmidt, B. Jurado, C. Amouroux and C. Schmitt, Nucl. Data Sheets **131**, 107 (2016)
12. D. A. Brown et al., Nucl. Data Sheets **148**, 1 (2018)